Isochronous partitions for region-based self-triggered control

Delimpaltadakis, I.; Mazo, M.

DOI
10.1109/TAC.2020.2994020

Publication date
2021

Document Version
Final published version

Published in
IEEE Transactions on Automatic Control

Isochronous Partitions for Region-Based Self-Triggered Control

Giannis Delimpaltadakis, *Student Member, IEEE*, and Manuel Mazo, Jr., *Senior Member, IEEE*

***Abstract*—In this article, we propose a *region-based* self-triggered control (STC) scheme for nonlinear systems. The state space is partitioned into a finite number of regions, each of which is associated to a uniform interevent time. The controller, at each sampling time instant, checks to which region does the current state belong, and correspondingly decides the next sampling time instant. To derive the regions along with their corresponding interevent times, we use approximations of *isochronous manifolds*, a notion first introduced in Anta and Tabuada (2012). This article addresses some theoretical issues of Anta and Tabuada (2012) and proposes an effective computational approach that generates approximations of isochronous manifolds, thus enabling the region-based STC scheme. The efficiency of both our theoretical results and the proposed algorithm is demonstrated through simulation examples.**

***Index Terms*—Digital control, networked control systems, nonlinear control systems.**

I. Introduction

CONTROL laws are, most often, implemented in a periodic fashion. However, despite periodic implementations facilitating controller design, they lead to overconsumption of available resources. Especially in networked control systems, such implementations are considered inefficient, due to potential limitations on communication bandwidth. The need for resource-friendly control implementations has shifted the research focus to aperiodic schemes, namely event-triggered control (ETC) [2]–[9] and self-triggered control (STC) [1], [10]–[21]. For an introduction to STC and ETC (see Heemels *et al.* [22]).

These strategies assume sample-and-hold implementations, in which the control action is updated when a certain performance-related condition (*triggering condition*) is satisfied. Triggering conditions are of the form $\phi(\zeta(t)) \geq 0$, where $\phi(\zeta(t))$ is a function of the state of the system, namely the *triggering function* (e.g., see Tabuada [4] and Girard [6]). Specifically in ETC, dedicated intelligent hardware constantly monitors the plant and detects when the triggering condition is satisfied. To relax this constraint, researchers have proposed STC as an alternative, according to which the controller predicts at each sampling time instant the next time at which the triggering condition would be satisfied. In this way, both ETC and STC promise to reduce the number of communication packets' transmissions and controller updates, thus saving both bandwidth and energy.

Regarding STC for nonlinear systems, the amount of published work is limited. In [11], the authors derive STC formulas employing interesting properties of homogeneous systems. Based on these properties, a different STC formula is proposed in [1], employing the notion of isochronous manifolds. In [12], a Taylor expansion of the Lyapunov function is used to predict the triggering times. In [16], a self-triggered scheme is derived, based on a small-gain approach. In [13], a triggering condition that guarantees uniform ultimate boundedness for perturbed nonlinear systems is presented, and a corresponding self-triggered sampler is derived. Finally, the work in [21] designs an STC scheme that copes with actuator delays.

The STC formula proposed in [11] proves to be conservative, i.e., it leads to a large amount of updates, at least when compared to the technique proposed here. This argument is illustrated in one of the simulation examples later in this document. In addition, Theodosis and Dimarogonas [21] admit that although it addresses actuator delays, it is even more conservative than Anta and Tabuada [11]. Regarding Anta and Tabuada [1], there are certain theoretical and practical issues that are presented later in this section and are thoroughly discussed in this document. An important drawback of the rest of the STC techniques is that they require heavy computations that need to be carried out online.

A clever way to provide a tradeoff between online computations and the number of updates in STC has already been proposed for linear systems with state feedback in [18]. In particular, the authors in [18] discretized the state space of a linear system into a finite number of regions, assigning a particular self-triggered interevent time to each region that lower bounds the event-triggered interevent times of all points contained in that region. The computation of the self-triggered interevent time for each region is carried out offline. Finally, in real-time, the controller checks to which region of the state space does the current state belong and assigns to it the interevent time of the corresponding region. To the best of our knowledge, there are no similar results for nonlinear systems.

Motivated by the advantages of Fiter *et al.* [18], in this article, we derive a *region-based* STC scheme for nonlinear systems. In contrast to the work in [18], in which the state space was

Manuscript received January 15, 2020; revised April 16, 2020; accepted May 6, 2020. Date of publication May 11, 2020; date of current version February 26, 2021. This work was supported by the ERC Starting Grant SENTIENT 755953. Recommended by Associate Editor A. Girard. *(Corresponding author: Giannis Delimpaltadakis.)*

The authors are with the Delft Center for Systems and Control, Delft University of Technology, 2628 CD Delft, The Netherlands (e-mail: i.delimpaltadakis@tudelft.nl; m.mazo@tudelft.nl).

Color versions of one or more of the figures in this article are available online at https://ieeexplore.ieee.org.

Digital Object Identifier 10.1109/TAC.2020.2994020

first discretized and afterward the corresponding self-triggered interevent times were computed, we propose to first predefine a set of specific interevent times and afterward derive the regions that correspond to the selected times. Thus, in our approach, the number of regions in the state space is always equal to the number of times. This renders our approach more efficient and tames the curse of dimensionality, as the number of regions is independent of the dimensions of the system.

Toward discretizing the state space of nonlinear systems, we elaborate on the notion of *isochronous manifolds*, originally introduced in [1]. Isochronous manifolds are hypersurfaces in the state space that consist of points associated to the same interevent time τ, i.e., if the system's state belongs to an isochronous manifold at a sampling time t_i, then the next sampling time instant is $t_{i+1} = t_i + \tau$. In [1], Anta and Tabuada proposed a method to approximate these manifolds by upper bounding the evolution of the triggering function, and then used the approximations to derive an STC formula. Unfortunately, there are some unaddressed theoretical and practical issues therein, which render the approximations, in general, invalid and hinder the application of the corresponding STC scheme. In particular, the bounding lemma presented in [1, Lemma V.2], based on which the upper bounds of the triggering function are derived, is incorrect. Furthermore, we show that even if a valid bound is obtained, the method proposed in [1] actually approximates the *zero-level sets of the triggering function*, and not the actual isochronous manifolds. Finally, although Anta and Tabuada [1] proposed the use of SOSTOOLS [23] to derive the approximations, we have found it to be numerically nonrobust regarding solving this particular problem.

This article tackles all of the aforementioned issues, in order to derive a discretization of the state space for nonlinear systems that enables a region-based STC scheme. Overall, the contributions of our article are the following.

1) We present a valid version of the bounding lemma, based on a higher order comparison lemma [24].
2) Employing this new lemma, we propose a refined methodology to approximate the actual isochronous manifolds of nonlinear ETC systems.
3) We adjust a counter-example guided iterative method (see e.g., [25]) combining linear programming and satisfiability modulo theory (SMT) solvers (e.g., [26]), to derive an alternative algorithm that effectively computes approximations of isochronous manifolds.
4) We derive a novel region-based STC scheme that provides a framework to tradeoff online computational load with the number of updates.

Finally, it is worth noting that isochronous manifolds are an inherent characteristic of any system with an output. Thus, as in [1], the theoretical contribution of deriving approximations of isochronous manifolds might even exceed the context in which this article is written.

II. Notation and Preliminaries

A. Notation

We denote points in $\mathbb{R}^n$ as x and their Euclidean norm as $|x|$. We use the symbol $\exists!$ to denote existence and uniqueness. For $x, y \in \mathbb{R}^n$, we write $x \preceq y$ if $x_i \leq y_i$ $(i = 1, \ldots, n)$, where the subscript i denotes the ith component of the corresponding vector. When there is no harm from ambiguity, the subscript i may be, also, used to denote different points $x_i \in \mathbb{R}^n$.

If $f : \mathbb{R}^n \to \mathbb{R}^m$ is p-times continuously differentiable, we write $f \in \mathcal{C}^p$. Let $X : M \to TM$ be a vector field and $h : M \to \mathbb{R}$ be a map. $\mathcal{L}_X h(x)$ denotes the Lie derivative of h at a point x along the flow of X. Similarly, $\mathcal{L}_X^k h(x) = \mathcal{L}_X(\mathcal{L}_X^{k-1} h(x))$ is the kth Lie derivative with $\mathcal{L}_X^0 h(x) = h(x)$.

Consider a system of first-order differential equations

$$\dot{\zeta}(t) = f(t, \zeta(t)). \tag{1}$$

The solution of (1) with initial condition ζ_0 and initial time t_0 is denoted as $\zeta(t; t_0, \zeta_0)$. When t_0 (and ζ_0) is clear from the context, then it is omitted, i.e., we write $\zeta(t; \zeta_0)$ $(\zeta(t))$.

B. ETC Systems

Consider a nonlinear control system

$$\dot{\zeta}(t) = f(\zeta(t), \upsilon(\zeta(t))) \tag{2}$$

where $\zeta : \mathbb{R} \to \mathbb{R}^n$, $f : \mathbb{R}^n \times \mathbb{R}^m \to \mathbb{R}^n$, and a feedback control law $\upsilon : \mathbb{R}^n \to \mathbb{R}^m$. A sample-and-hold implementation of (2) is typically applied by sampling the state of the system $\zeta(t)$ at time instants t_i, $i = 0, 1, 2, \ldots$, evaluating the input $\upsilon(\zeta(t_i))$ and keeping it constant until the next sampling time

$$\dot{\zeta}(t) = f(\zeta(t), \upsilon(\zeta(t_i))), \quad t \in [t_i, t_{i+1}).$$

We define the measurement error $\varepsilon(t)$ as the difference between the last measured state and the current state

$$\varepsilon(t) := \zeta(t_i) - \zeta(t), \quad t \in [t_i, t_{i+1}). \tag{3}$$

As soon as the updated control input is applied at each sampling time $t = t_i$, the state is measured and the error becomes 0, since $\zeta(t) = \zeta(t_i)$. With this definition, the sample-and-hold closed loop becomes

$$\dot{\zeta}(t) = f(\zeta(t), \upsilon(\varepsilon(t) + \zeta(t))). \tag{4}$$

In ETC, the sampling time instants, or *triggering times*, are defined as follows:

$$t_{i+1} = t_i + \inf\{t > 0 : \phi(\zeta(t; x_i), \varepsilon(t; 0)) = 0\} \tag{5}$$

and $t_0 = 0$, where x_i corresponds to the last measurement of the state of the plant. We call (5) the *triggering condition*, $\phi(\cdot, \cdot)$ the *triggering function*, and the difference $t_{i+1} - t_i$ *inter-event time*. Each point x_i in the state space of the system corresponds to a specific interevent time denoted by $\tau(x_i)$

$$\tau(x_i) := \inf\{t > 0 : \phi(\zeta(t; x_i), \varepsilon(t; 0)) = 0\}. \tag{6}$$

During the interval $[t_i, t_{i+1})$, the triggering function starts from a negative value and remains negative until t_{i+1}. At t_{i+1}, it becomes zero. Typically, it is designed such that $\phi(\zeta(t; x_i), \varepsilon(t; 0)) \leq 0$ implies certain stability guarantees for the system. This justifies the choice (5) of sampling times.

If we consider the extended state vector $\xi(t) = \begin{bmatrix} \zeta^\top(t) & \varepsilon^\top(t) \end{bmatrix}^\top \in \mathbb{R}^{2n}$, the ETC system is written

in a compact way

$$\dot{\xi}(t) = \begin{bmatrix} f(\zeta(t), \upsilon(\zeta(t)+\varepsilon(t)) \\ -f(\zeta(t), \upsilon(\zeta(t)+\varepsilon(t)) \end{bmatrix} = F(\xi(t)),\ t \in [t_i, t_{i+1})$$
$$\xi_1(t_{i+1}^+) = \xi_1(t_{i+1}^-)$$
$$\xi_2(t_{i+1}^+) = 0. \tag{7}$$

Remark 1: Our analysis is carried out within the time interval $[0, t_{i+1} - t_i) = [0, \tau(x_i))$. Due to time-invariance of $F(\cdot), \phi(\cdot)$, this is equivalent to analyzing within the interval $[t_i, t_{i+1})$.

At any sampling time t_i, the state of (7) becomes $\xi(t_i) = (\zeta(t_i), 0) = (x_i, 0)$. Since we consider intervals between two sampling times, we focus on solutions $\xi(t; \xi_i)$ with $\xi_i = (x_i, 0)$. Thus, we adopt the abusive notation $\phi(\xi(t; x_i))$, $\tau(x_i)$ (or later $\psi(x_i, t)$, $\mu(x_i, t)$) instead of $\phi(\xi(t; \xi_i))$, $\tau(\xi_i)$.

C. Self-Triggered Implementation

As aforementioned, self-triggered implementations remove the need for continuous monitoring of the triggering condition (5), by predicting events $\phi(\xi(t; x)) = 0$. Specifically, an STC strategy dictates the next sampling time according to a function $\tau^{\downarrow} : \mathbb{R}^n \to \mathbb{R}^+$ lower bounding the ETC interevent times

$$\tau^{\downarrow}(x) \leq \tau(x). \tag{8}$$

Since $\phi(\xi(t; x)) < 0$ for all $t \in [0, \tau(x))$, then it is guaranteed that $\phi(\xi(t; x)) < 0$ for all $t \in [0, \tau^{\downarrow}(x))$, and the stability of the system is preserved. Consequently, the STC interevent times should be no larger than the corresponding ETC times in order to guarantee stability, but as large as possible in order to achieve greater reduction of updates. Finally, $\tau^{\downarrow}(\cdot)$ should be designed such that $\tau^{\downarrow}(x) \geq \epsilon > 0$ for all x in the operating region of the system, in order to avoid the scenario of infinite transmissions in finite amount of time (Zeno phenomenon).

III. Problem Statement

Inspired by the work in [18], the goal of this article is to design a region-based STC scheme for nonlinear systems, providing a framework for tradeoff between online computations and updates. In a region-based STC scheme, the state space of the original system (4) is divided into a finite number of regions $\mathcal{R}_i \in \mathbb{R}^n$ $(i = 1, 2, \dots)$, each of which is associated to a self-triggered interevent time τ_i such that

$$\forall x \in \mathcal{R}_i : \quad \tau_i \leq \tau(x) \tag{9}$$

where $\tau(x)$ denotes the event-triggered interevent time associated to x [see (6)]. The STC scheme operates as follows.

1) Measure the current state $\xi(t_k) = (x_k, 0)$.
2) Check to which of the regions $\mathcal{R}_i$ does x_k belong.
3) If $x_k \in \mathcal{R}_i$, set the next sampling time to $t_{k+1} = t_k + \tau_i$.

The STC scheme preserves stability of the system, since the STC interevent times lower bound the ETC ones [see (9)].

In [18], the state space is discretized into regions $\mathcal{R}_i$ *a priori*, and afterward the times τ_i are computed such that they satisfy (9). However, we propose an alternative approach: first, a finite set of times $\{\tau_1, \tau_2, \dots \tau_q\}$ is *predefined* (e.g., by the user), which will serve as STC interevent times, with $\tau_i < \tau_{i+1}$, and then regions $\mathcal{R}_i$ corresponding to times τ_i are derived *a posteriori*, such that (9) is satisfied. In this way, the number of regions is equal to the number of times τ_i, in contrast to the work in [18], and the curse of dimensionality is tamed, as the number of regions does not depend on the system's dimensionality. Thus, the problem statement is as follows.

Problem Statement Given a finite set of times $\{\tau_1, \dots \tau_q\}$, with $\tau_i < \tau_{i+1}$ and $q > 1$, find $\mathcal{R}_i \in \mathbb{R}^n$ that satisfy (9).

Note that Zeno behavior is ruled out by construction, since the STC interevent times are lower bounded: $\tau^{\downarrow}(x) \geq \min_i\{\tau_i\} = \tau_1$. The choice of times τ_i and its effect is discussed later in this document.

IV. Isochronous Manifolds, Triggering Level Sets, and Discretization

Here, we recall results from Anta and Tabuada [1] regarding isochronous manifolds, we introduce the notion of *triggering level sets* and describe how isochronous manifolds and triggering level sets are different. Finally, we point out how, given proper approximations of isochronous manifolds, a state-space discretization is generated, enabling a region-based STC scheme.

A. Homogeneous Systems and Scaling of Interevent Times

First, we briefly go through some definitions regarding homogeneous functions and systems, and results previously derived in [11] regarding scaling laws for interevent times of homogeneous systems. Regarding the former, only the classical notion of homogeneity is presented. For the general definition of homogeneity, the reader is referred to Kawski [27].

Definition IV.1 (Homogeneous Function [1]): A function $f : \mathbb{R}^n \to \mathbb{R}^m$ is homogeneous of degree $\alpha \in \mathbb{N}$, if there exist $r_i > 0$ $(i = 1, 2, \dots, m)$ such that for all $x \in \mathbb{R}^n$

$$f_i(\lambda^{r_1} x_1, \dots, \lambda^{r_n} x_n) = \lambda^{\alpha + r_i} f_i(x_1, \dots, x_n) \quad \forall \lambda > 0$$

where $f_i(x)$ is the ith component of $f(x)$ and $\alpha > -\min_i r_i$.

Definition IV.2 (Homogeneous System): A system (2) is called homogeneous of degree $\alpha \in \mathbb{R}$, whenever $f(\zeta(t), \upsilon(\zeta(t))) = \tilde{f}(\zeta(t))$ is a homogeneous function of the same degree.

We now review the scaling laws of interevent times previously derived in [11]. Along lines passing through the origin (but excluding the origin), the event-triggered interevent times scale according to the following rule.

Theorem IV.1 (Scaling Law [11]): Consider a dynamical system (7) homogeneous of degree α and a triggering function $\phi(\cdot)$ homogeneous of degree θ. For all $x \in \mathbb{R}^n$, the interevent times $\tau : \mathbb{R}^n \to \mathbb{R}^+ \cup \{+\infty\}$ defined by (6) scale as

$$\tau(\lambda x) = \lambda^{-\alpha} \tau(x), \quad \lambda > 0. \tag{10}$$

In the following, we refer to lines going through the origin as *homogeneous rays*. Notice that the scaling law for the interevent times (10) does not depend on the degree of homogeneity of the triggering function considered. The property derives from the following useful lemma.

Lemma IV.2 (Time-Scaling Property [11]): Consider an ETC system (7) and a triggering function $\phi(\cdot)$ homogeneous of degree α and θ, respectively. The triggering function satisfies

$$\phi(\xi(t;\lambda x)) = \phi(\lambda\xi(\lambda^{\alpha}t;x)) = \lambda^{\theta+1}\phi(\xi(\lambda^{\alpha}t;x)) \qquad (11)$$

where the first equality is a property of homogeneous flows.

Assumption 1: For the remaining of this article, our analysis is based on the following set of assumptions.

1) The extended ETC system (7) is smooth and homogeneous of degree $\alpha \geq 1$, with $r_i = 1$ for all i.
2) The triggering function $\phi(\xi(t;x))$ is smooth and homogeneous of degree $\theta \geq 1$, with $r_i = 1$ for all i.
3) For all $x \in \mathbb{R}^n - \{0\}$, $\phi(\xi(0;x)) < 0$ and $\exists t_x \in (0,+\infty)$ such that $\phi(\xi(t_x;x)) = 0$.
4) Compact sets $\mathrm{Z} \subset \mathbb{R}^n$ and $\Xi \subset \mathbb{R}^{2n}$, containing a neighborhood of the origin, are given, such that for all $x \in \mathrm{Z}$: $\phi(\xi(t;x)) \leq 0 \Rightarrow \xi(t;x) \in \Xi$.
5) The system (2) has the origin as the only equilibrium.

Remark 2: The aforementioned analysis and Assumption 1 constitute the framework within which this article is carried out. Nevertheless, as pointed out in [1, Lemma IV.4], any smooth function can be rendered homogeneous, if embedded in a higher dimensional space. Thus, our results are applicable to general smooth nonlinear systems and triggering functions. This is thoroughly discussed in Appendix D and showcased in Section VII-B via a numerical example.

Remark 3: The set Ξ could be $\Xi = \mathrm{Z} \times \mathrm{E}$, where $\mathrm{Z} = \{x \in \mathbb{R}^n : V(x) \leq c\}$, $\mathrm{E} = \{x_0 - x \in \mathbb{R}^n : x, x_0 \in \mathrm{Z}\}$, $c > 0$, and $V(\cdot)$ is a radially unbounded Lyapunov function for the ETC system. In most ETC schemes (e.g., [4]), $V(x)$ is given and the triggering function satisfies: $\phi(\xi(t;x)) \leq 0 \Rightarrow \dot{V}(\zeta(t;x)) \leq 0$. Thus, trajectories of (7) starting from $\mathrm{Z} \times \{0\} \subset \Xi$ stay in $\Xi = \mathrm{Z} \times \mathrm{E}$. The intuition behind this assumption is analyzed in Section V-C. An alternative way of constructing Z and Ξ is demonstrated in Section VII-B.

B. Isochronous Manifolds and Triggering Level Sets

Definition IV.3 (Isochronous Manifolds): Consider a closed-loop system (7) and a triggering function $\phi(\cdot)$. The set $M_{\tau_\star} = \{x \in \mathbb{R}^n : \tau(x) = \tau_\star\}$, where $\tau(x)$ is defined by (6), is called an isochronous manifold of time $\tau_\star$.

Alternatively, all points $x \in \mathbb{R}^n$ that correspond to interevent time $\tau_\star$ constitute the isochronous manifold $M_{\tau_\star}$. Isochronous manifolds are of dimension $n-1$ (proven in [1]).

Definition IV.4 (Triggering Level Sets): We call the set

$$L_{\tau_\star} := \{x \in \mathbb{R}^n : \phi(\xi(\tau_\star;x)) = 0\} \qquad (12)$$

triggering level set of $\phi(\xi(\tau_\star;x))$ for time $\tau_\star$.

Triggering level sets are the zero-level sets of the triggering function, for fixed t. Let us now make a crucial observation: *The equation $\phi(\xi(t;x)) = 0$ may have multiple solutions with respect to time t for a given x.* In other words, there might exist points $x \in \mathbb{R}^n$ and time instants $\tau_{x,1} < \tau_{x,2} < \ldots < \tau_{x,k}$, with $k > 1$ such that $\phi(\xi(\tau_{x,i};x)) = 0$ for all $i = 1, 2, \ldots, k$. We briefly present an example with a triggering function exhibiting multiple zero crossings for given initial conditions.

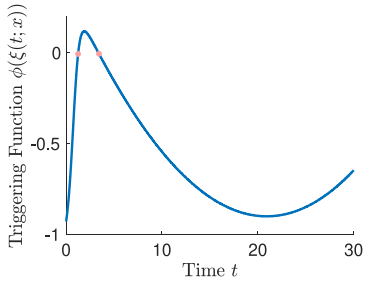

Fig. 1. Time evolution of $\phi(x;t)$ for initial condition $[-0.5,-1]^\top$. It exhibits multiple zero crossings.

Example: Consider the jet-engine compressor control system from [28]

$$\dot{\xi}_1(t) = -\xi_2(t) - \frac{3}{2}\xi_1^2(t) - \frac{1}{2}\xi_1^3(t), \quad \dot{\xi}_2(t) = \upsilon(\xi(t))$$

with control law $\upsilon(\xi(t)) = \xi_1(t) - \frac{1}{2}(\xi_1^2(t)+1)(y + \xi_1^2(t)y + \xi_1(t)y^2) + 2\xi_1(t)$, where $y = 2\frac{\xi_1^2+\xi_2}{\xi_1^2+1}$. A triggering function that guarantees asymptotic stability is the following [11]:

$$\phi(\xi(t;x)) = |\varepsilon|^2 - 0.82\sigma^2|\xi(t;x)|^2, \qquad \sigma \in (0,1).$$

The evolution of the triggering function $\phi(\xi(t;x))$ for the initial condition $[-0.5\ -1]^\top$ is simulated and illustrated in Fig. 1. It is clear from the figure that it exhibits multiple zero crossings, for $t = \tau_{x,1} \approx 1.15$ s and $t = \tau_{x,2} \approx 3.22$ s. ■

Interevent times are defined as *the first zero crossing of the triggering function* [see (6)], i.e., $\tau(x) = \tau_{x,1}$. Isochronous manifolds are defined with respect to this first zero crossing, and any point $x \in \mathbb{R}^n - \{0\}$ belongs only to one isochronous manifold: $M_{\tau_{x,1}}$. However, the same point belongs to all triggering level sets $L_{\tau_{x,i}}$. For instance, in the previous example, the point $x = (-0.5,-1)$ belongs to both triggering level sets $L_{1.15}$ and $L_{3.22}$, whereas it belongs to only one isochronous manifold, i.e., $M_{1.15}$. In [1], isochronous manifolds and triggering level sets are treated as if they were identical, which creates problems regarding approximating isochronous manifolds. This is addressed later in this document.

Remark 4: If the triggering function $\phi(\xi(t;x))$ has only one zero crossing for all $x \in \mathbb{R}^n - \{0\}$, then the triggering level sets do coincide with the isochronous manifolds, i.e., $M_{\tau_\star} = \{x \in \mathbb{R}^n : \tau(x) = \tau_\star\} = \{x \in \mathbb{R}^n : \phi(\xi(\tau_\star;x)) = 0\} = L_{\tau_\star}$.

Isochronous manifolds possess the two following properties.

Proposition IV.1 (see [1]): Consider an ETC system (7), a triggering function $\phi(\cdot)$, and let Assumption 1 holds. Each homogeneous ray intersects any isochronous manifold only at one point

$$\forall \tau_\star > 0 \text{ and } \forall x \in \mathbb{R}^n - \{0\} : \exists! \lambda_x > 0 \text{ such that } \lambda_x x \in M_{\tau_\star}. \qquad (13)$$

Proof: According to (10) and (11), on any homogeneous ray, times vary from 0 to $+\infty$ as λ_x varies from $+\infty$ to 0. Thus, for any $\tau_\star \in \mathbb{R}^+$, there exists a point x on each ray such that $\tau(x) = \tau_\star$. In addition, (10) implies that there do not exist two different points on the same homogeneous ray that correspond to the same interevent time.

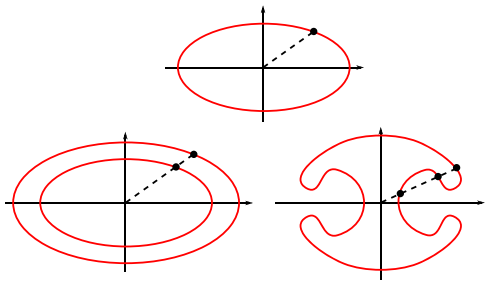

Fig. 2. Curve on the top is intersected only once by each homogeneous ray, thus it could be an isochronous manifold of a homogeneous system. The two bottom curves are intersected by some homogeneous rays more than once, thus they cannot be isochronous manifolds of a homogeneous system.

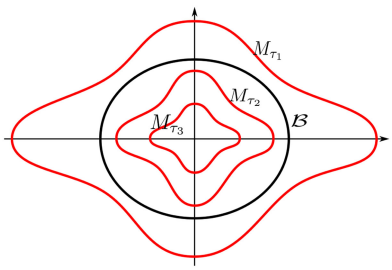

Fig. 3. Isochronous manifolds M_{τ_1}, M_{τ_2}, and M_{τ_3} (red lines) for $\tau_1 < \tau_2 < \tau_3$, and the operating region $\mathcal{B}$ (black line).

Proposition IV.2: Consider an ETC system (7), a triggering function $\phi(\cdot)$, and let Assumption 1 holds. Consider isochronous manifolds M_{τ_i} and $M_{\tau_{i+1}}$, with $\tau_i < \tau_{i+1}$. The following holds for all $x \in M_{\tau_i}$:

$$\exists! \lambda_x \in (0,1) \text{ s.t. } \lambda_x x \in M_{\tau_{i+1}} \wedge \nexists \kappa_x \geq 1 \text{ s.t. } \kappa_x x \in M_{\tau_{i+1}}. \tag{14}$$

Proof: According to Proposition IV.1, since each homogeneous ray intersects any isochronous manifold only at one point, $\exists! \lambda_x > 0$ such that $\lambda_x x \in M_{\tau_{i+1}}$, where $x \in M_{\tau_i}$. From the scaling law (10), we get

$$\tau_{i+1} = \tau(\lambda_x x) = \lambda_x^{-\alpha} \tau_i \Rightarrow \lambda_x = \sqrt[\alpha]{\left(\frac{\tau_i}{\tau_{i+1}}\right)} < 1$$

since $\tau_i < \tau_{i+1}$. There can be no other intersection of the homogeneous ray with $M_{\tau_{i+1}}$, i.e., $\nexists \kappa_x \geq 1$ s.t. $\kappa_x x \in M_{\tau_{i+1}}$. ■

Proposition IV.2 states that isochronous manifolds for smaller times are further away from the origin. Given (13), in Fig. 2, the curve on the top could be an isochronous manifold of a homogeneous system, whereas the two bottom curves cannot.

Remark 5: Properties (13) and (14) of isochronous manifolds result directly from the time scaling property (11).

C. State-Space Discretization and a Self-Triggered Strategy

For the following, we assume that the system operates in an arbitrarily large compact set $\mathcal{B}$ the whole time. Assume that isochronous manifolds M_{τ_i} for $\tau_1 < \tau_2 < \tau_3$ are given, as illustrated in Fig. 3. We define the regions between manifolds as

$$R_i = \{x \in \mathbb{R}^n : \exists \kappa_x \geq 1 \text{ s.t. } \kappa_x x \in M_{\tau_i} \wedge \exists \lambda_x \in (0,1) \text{ s.t. } \lambda_x x \in M_{\tau_{i+1}}\} \tag{15}$$

for $\tau_i < \tau_{i+1}$, and the region enclosed by the manifold M_{τ_3} as $R_3 = \{x \in \mathbb{R}^n : \exists \kappa_x \geq 1 \text{ s.t. } k_x x \in M_{\tau_3}\}$. Since (14) holds, a region R_i is the set with its outer boundary being M_{τ_i} and its inner boundary being $M_{\tau_{i+1}}$. The scaling law (10) implies that: $\tau(x) \geq \tau_i$ for all $x \in R_i$. Thus, isochronous manifolds could be employed for discretizing the state space in regions R_i such that (9) is satisfied. If isochronous manifolds did not satisfy property (13), then the regions R_i could potentially intersect with each other (see Fig. 4). Hence, it would not be possible to derive a discretization as the one described.

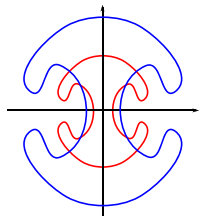

Fig. 4. If isochronous manifolds did not satisfy (13), it would not be possible to discretize the state space enabling a region-based STC scheme.

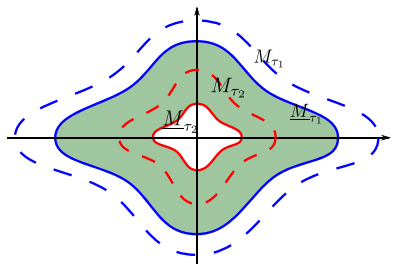

Fig. 5. Isochronous manifolds M_{τ_i} (dashed lines) and their inner approximations $\underline{M}_{\tau_i}$ (solid lines). The filled region represents $\mathcal{R}_1$.

D. Inner Approximations of Isochronous Manifolds and Discretization

Deriving the actual isochronous manifolds is generally not possible, as nonlinear systems most often do not admit a closed-form analytical solution. Thus, in order to discretize the state space and generate a region-based STC scheme, we propose a method to construct inner approximations of isochronous manifolds, as shown in Fig. 5.

Definition IV.5 (Inner Approximations of Isochronous Manifolds): Consider a system (7) and a triggering function, and let Assumption 1 holds. A set $\underline{M}_{\tau_i}$ is called inner approximation of an isochronous manifold M_{τ_i} if and only if for all $x \in \underline{M}_{\tau_i}$

$$\exists \kappa_x \geq 1 \text{ s.t. } \kappa_x x \in M_{\tau_i} \text{ and } \nexists \lambda_x \in (0,1) \text{ s.t. } \lambda_x x \in M_{\tau_i}. \tag{16}$$

In other words, an inner approximation of an isochronous manifold is contained inside the region encompassed by the

isochronous manifold. Consider inner approximations $\underline{M}_{\tau_i}$ of isochronous manifolds ($\tau_1 < \tau_2 < \dots$) that satisfy properties (13) and (14). We consider the regions between sets $\underline{M}_{\tau_i}$

$$\mathcal{R}_i = \{x \in \mathbb{R}^n : \exists \kappa_x \geq 1 \text{ s.t. } \kappa_x x \in \underline{M}_{\tau_i} \wedge \exists \lambda_x \in (0,1) \text{ s.t. } \lambda_x x \in \underline{M}_{\tau_{i+1}}\}. \tag{17}$$

A region $\mathcal{R}_i$ is the set with its outer boundary being $\underline{M}_{\tau_i}$ and its inner boundary being $\underline{M}_{\tau_{i+1}}$ (see Fig. 5). For such sets, by (10) we get the following result.

Corollary IV.1: Consider a system (7) and a triggering function $\phi(\cdot)$, and let Assumption 1 holds. Consider two inner approximations $\underline{M}_{\tau_i}$ and $\underline{M}_{\tau_{i+1}}$ of isochronous manifolds, with $\tau_i \leq \tau_{i+1}$. Assume that $\underline{M}_{\tau_i}$ and $\underline{M}_{\tau_{i+1}}$ satisfy (13) and (14). For the region $\mathcal{R}_i$ defined in (17), the following holds:

$$\forall x \in \mathcal{R}_i : \tau_i \leq \tau(x).$$

Proof: For all $x \in \mathcal{R}_i$, $\exists \kappa_x \geq 1$ s.t. $\kappa_x x \in \underline{M}_{\tau_i}$. Thus, $\exists k_x \geq \kappa_x \geq 1$ s.t. $k_x x \in M_{\tau_i}$. By (10), we have $\tau(k_x x) = \tau_i \Rightarrow \tau(x) = k_x^{\alpha} \tau_i \geq \tau_i$. ■

Thus, given inner approximations of isochronous manifolds, the state space can be discretized into regions $\mathcal{R}_i$, enabling the region-based STC scheme. *This construction requires that inner approximations should also satisfy (13) and (14). Deriving inner approximations $\underline{M}_{\tau_\star}$ of isochronous manifolds such that they satisfy (13) and (14) constitutes the main theoretical challenge of this article.*

Remark 6: As already noted, the number of regions $\mathcal{R}_i$ equals the number q of predefined times τ_i (see Section III). Given that τ_1 and τ_q are fixed, as the number of times q grows, the areas of regions $\mathcal{R}_i$ become smaller, as the same space is discretized into more regions. Thus, the STC interevent times τ_i become more accurate bounds of the actual ETC times $\tau(x)$. However, during the online implementation, the controller in general needs to perform more checks to determine the region of a measured state. Hence, the number q of times τ_i provides a tradeoff between computations and conservativeness.

Remark 7: Note that τ_1 has to be selected, such that the operating region $\mathcal{B}$ lies completely inside the region delimited by $\underline{M}_{\tau_1}$ (see e.g., Fig. 3). To check this, the approach of [11] or an SMT solver (e.g., [26]) can be used.

Remark 8: For nonhomogeneous systems, there will always exist a neighborhood around the origin that cannot be contained in any region $\mathcal{R}_i$. However, this set can be made arbitrarily small, by selecting a sufficiently small time τ_1. For a thorough discussion on this, the reader is referred to Appendix D.

V. Approximations of Isochronous Manifolds

Here, a refined methodology is presented, which generates inner approximations of isochronous manifolds that satisfy (13) and (14). First, we show how the method of Anta and Tabuada [1] actually approximates triggering level sets, and then we refine its core idea to derive approximations of isochronous manifolds.

A. Approximations of Triggering Level Sets

The method proposed in [1] is based on bounding the time evolution of the triggering function by another function with linear dynamics: $\psi_1(x,t) \geq \phi(\xi(t;x))$, with $\psi_1(x,0) = \phi(\xi(0;x)) < 0$ for all $x \in \mathbb{R}^n - \{0\}$. The bound is obtained by constructing a linear system according to a bounding lemma ([1, Lemma V.2]). Unfortunately, this lemma is invalid and the function that is obtained does not always bound $\phi(\xi(t;x))$. Specifically, a counterexample is given in [29, p. 2, Example 2]. However, later in this document, we present a slightly adjusted lemma that is actually valid. Thus, for this section, we assume that $\psi_1(x,t)$ is an upper bound of $\phi(\xi(t;x))$.

Since $\psi_1(x,t) \geq \phi(\xi(t;x))$ and $\psi_1(x,0) < 0$, if we define

$$\tau^{\downarrow}(x) = \inf\{t > 0 : \psi_1(x,t) = 0\}$$

then it is guaranteed that $\phi(\xi(x;t)) \leq 0 \quad \forall t \in [0, \tau^{\downarrow}(x)]$. Hence, the first zero crossing of $\psi_1(x,t)$ for a given x happens before the first zero crossing of $\phi(\xi(t;x))$, i.e., the interevent time of x is lower bounded by $\tau^{\downarrow}(x)$: $\tau(x) \geq \tau^{\downarrow}(x)$.

In [1], under the misconception that isochronous manifolds and triggering level sets coincide, it is argued that to approximate an isochronous manifold, it suffices to approximate the set $L_{\tau_\star} := \{x \in \mathbb{R}^n : \phi(\xi(\tau_\star;x)) = 0\}$, i.e., a triggering level set. Thus, the upper bound $\psi_1(x,t)$ of $\phi(\xi(t;x))$ is used to derive the following approximation: $\underline{L}_{\tau_\star} := \{x \in \mathbb{R}^n : \psi_1(x,\tau_\star) = 0\}$. However, as we have already pointed out for the triggering function, $\psi_1(x,t)$ might also have multiple zero crossings for a given $x \in \mathbb{R}^n$. Thus, the equation $\psi_1(x,t) = 0$ does not only capture the interevent times of points x, but possibly also more zero crossings of $\phi(t;x)$. Thus, we can say that the set $\underline{L}_{\tau_\star}$ is an approximation of the triggering level set $L_{\tau_\star}$, and not of the isochronous manifold $M_{\tau_\star}$. Furthermore, observe that $\psi_1(x,t)$ does not *a priori* satisfy the time scaling property (11). Consequently, there is no formal guarantee that the sets $\underline{L}_{\tau_\star}$ satisfy (13) (see Remark 5). In other words, the sets $\underline{L}_{\tau_\star}$ might be intersected by some homogeneous rays more than once, or they may not be intersected at all.

Remark 9: In [1], given a fixed time $\tau_\star$, the equation

$$\psi_1(\tfrac{x_0}{\lambda}, \tau_\star) = 0 \tag{18}$$

is solved w.r.t. λ, in order to determine the STC interevent time of the measured state x_0 as: $\tau^{\downarrow}(x_0) = \lambda^{-\alpha}\tau_\star$. Note that (18) finds intersections $\frac{x_0}{\lambda}$ of $\underline{L}_{\tau_\star}$ with the ray passing through x_0. Hence, the aforementioned observations imply that (18) may not have any real solution, or may admit some solutions λ such that $\tau^{\downarrow}(x_0) = \lambda^{-\alpha}\tau_\star > \tau(x)$, hindering stability.

B. Inner Approximations of Isochronous Manifolds

Although, the method of Anta and Tabuada [1] generates approximations of triggering level sets, which do not satisfy (13), we employ the idea of upper bounding the triggering function, and we impose additional properties to the upper bound, such that the obtained sets approximate isochronous manifolds and satisfy (13) and (14). Remarks 4 and 5 state that: first, isochronous manifolds coincide with triggering level sets, if $\phi(\cdot)$ has only one zero crossing w.r.t. t, and second, $\phi(\cdot)$ satisfying (11) implies that isochronous manifolds satisfy (13) and (14). Intuitively, we could construct a function $\mu(x,t)$ that satisfies the same properties and its zero crossing happens before the one of $\phi(\cdot)$, and use the level sets $\underline{M}_{\tau_\star} = \{x \in \mathbb{R}^n : \mu(x,\tau_\star) = 0\}$ as

inner approximations of isochronous manifolds that satisfy (13) and (14). The aforementioned are summarized in the following theorem.

Theorem V.1: Consider an ETC system (7), a triggering function $\phi(\cdot)$, and let Assumption 1 holds. Let $\mu : \mathbb{R}^n \times \mathbb{R}^+ \to \mathbb{R}$ be a function that satisfies

$$\mu(x,0) < 0 \quad \forall x \in \mathbb{R}^n - \{0\}, \tag{19a}$$

$$\mu(x,t) \geq \phi(\xi(t;x)) \quad \forall t \in [0, \tau(x)] \text{ and } \quad \forall x \in \mathbb{R}^n - \{0\} \tag{19b}$$

$$\mu(\lambda x, t) = \lambda^{\theta+1} \mu(x, \lambda^{\alpha} t) \quad \forall t, \lambda > 0 \text{ and } \quad \forall x \in \mathbb{R}^n - \{0\} \tag{19c}$$

$$\forall x \in \mathbb{R}^n - \{0\} : \quad \exists! \tau_x \text{ such that } \mu(x, \tau_x) = 0. \tag{19d}$$

The sets $\underline{M}_{\tau_\star} = \{x \in \mathbb{R}^n : \mu(x, \tau_\star) = 0\}$ are inner approximations of isochronous manifolds $M_{\tau_\star}$ and satisfy (13) and (14).

Proof: See the Appendix. ∎

Remark 10: It is crucial that inequality (19b) extends at least until $\tau(x)$, in order for $\mu(x,t)$ to capture the actual interevent time, i.e., for the minimum time satisfying $\mu(x,t) = 0$ to lower bound the minimum time satisfying $\phi(\xi(t;x)) = 0$.

C. Constructing the Upper Bound of the Triggering Function

In this section, we construct a valid bounding lemma and we employ it in order to derive an upper bound $\mu(x,t)$ of the triggering function $\phi(\xi(t;x))$, such that it satisfies (19).

Lemma V.2: Consider a system of differential equations $\dot{\xi}(t) = F(\xi(t))$, where $\xi : \mathbb{R}^+ \to \mathbb{R}^n$, $F : \mathbb{R}^n \to \mathbb{R}^n$, a function $\phi : \mathbb{R}^n \to \mathbb{R}$, and a set $\Omega_d = \{x \in \mathbb{R}^n : |x| < d\}$. For every set of coefficients $\delta_0, \delta_1, \ldots, \delta_p \in \mathbb{R}^+$ satisfying

$$\mathcal{L}_F^p \phi(z) \leq \sum_{i=0}^{p-1} \delta_i \mathcal{L}_F^i \phi(z) + \delta_p \quad \forall z \in \Omega_d \tag{20}$$

the following inequality holds for all $\xi_0 \in \Omega_d$:

$$\phi(\xi(t;\xi_0)) \leq \psi_1(y(\xi_0), t) \quad \forall t \in [0, \tau_{\xi_0})$$

where τ_{ξ_0} is defined as

$$\tau_{\xi_0} = \sup\{\tau > 0 : \xi(t;\xi_0) \in \Omega_d \quad \forall t \in [0,\tau)\} \tag{21}$$

and $\psi_1(y(\xi_0), t)$ is the first component of the solution of the following linear dynamical system:

$$\dot{\psi} = \begin{bmatrix} 0 & 1 & 0 & \ldots & 0 & 0 \\ 0 & 0 & 1 & \ldots & 0 & 0 \\ \vdots & \vdots & & \ddots & \vdots & \vdots \\ 0 & 0 & 0 & \ldots & 1 & 0 \\ \delta_0 & \delta_1 & \delta_2 & \ldots & \delta_{p-1} & 1 \\ 0 & 0 & 0 & \ldots & 0 & 0 \end{bmatrix} \psi = A\psi \tag{22}$$

with initial condition

$$y(\xi_0) = \begin{bmatrix} \phi(\xi_0) & \mathcal{L}_F \phi(\xi_0) & \ldots & \mathcal{L}_F^{p-1} \phi(\xi_0) & \delta_p \end{bmatrix}^\top.$$

Proof: See the Appendix. ∎

Remark 11: The main difference between Lemma V.2 and the bounding lemma in [1] is that in Lemma V.2, the coefficients δ_i are forced to be nonnegative. We also include a proof, employing a higher order comparison lemma, since the comparison lemma arguments used in the proof of Anta and Tabuada[1] are invalid.

Let us define the open ball

$$\Omega_d := \{x \in \mathbb{R}^{2n} : |x| < d\}. \tag{23}$$

Consider the following feasibility problem.

Problem 1: Consider a system (7) and a triggering function $\phi(\cdot)$ and let Assumption 1 holds. Find $\delta_0, \ldots, \delta_p \in \mathbb{R}$ such that

$$\mathcal{L}_F^p \phi(z) \leq \sum_{i=0}^{p-1} \delta_i \mathcal{L}_F^i \phi(z) + \delta_p \quad \forall z \in \Omega_d \tag{24a}$$

$$\delta_0 \phi\left((x,0)\right) + \delta_p \geq \epsilon > 0 \quad \forall x \in \mathrm{Z} \tag{24b}$$

$$\delta_i \geq 0, \quad i = 0, 1, \ldots, p \tag{24c}$$

where ϵ is an arbitrary predefined positive constant, d is such that $\Xi \subset \Omega_d$, and Z, Ξ and Ω_d are given by Assumption 1 and (23), respectively.

The feasible solutions of (24) belong in a subset of the feasible solutions of Lemma V.2, i.e., the solutions of (24) determine upper bounds of the triggering function. Moreover, such δ_i always exist, since to satisfy (24) it suffices to pick $\delta_p \geq \max\{\epsilon, \sup_{z \in \Omega_d} \mathcal{L}_F^p \phi(z)\}$ and $\delta_i = 0$ for $i = 0, \ldots, p-1$. The following theorem shows how to employ solutions of Problem 1, in order to construct upper bounds that satisfy (19).

Theorem V.3: Consider a system (7), a triggering function $\phi(\cdot)$, and coefficients $\delta_0, \ldots, \delta_p$ solving Problem 1. Let Assumption 1 holds. Let $D = \{x \in \mathbb{R}^n : |x| = r\}$, with $r > 0$ and $D \subset \mathrm{Z}$. Define the following function for all $x \in \mathbb{R}^n - \{0\}$:

$$\mu(x,t) := C\left(\tfrac{|x|}{r}\right)^{\theta+1} e^{A\left(\frac{|x|}{r}\right)^{\alpha} t} \begin{bmatrix} \phi\left(\left(r\frac{x}{|x|}, 0\right)\right) \\ \max\left(\mathcal{L}_f \phi\left(\left(r\frac{x}{|x|}, 0\right)\right), 0\right) \\ \vdots \\ \max\left(\mathcal{L}_f^{p-1} \phi\left(\left(r\frac{x}{|x|}, 0\right)\right), 0\right) \\ \delta_p \end{bmatrix} \tag{25}$$

where A is as in (22), $C = [1\ 0\ \ldots\ 0]$, and α and θ are the degrees of homogeneity of the system and the triggering function, respectively. The function $\mu(x,t)$ satisfies (19).

Proof: See the Appendix. ∎

Thus, according to Theorem V.1, the sets $\underline{M}_{\tau_\star} = \{x \in \mathbb{R}^n : \mu(x, \tau_\star) = 0\}$ are inner approximations of the actual isochronous manifolds of the system and satisfy (13) and (14). The fact that $\mu(x,t)$ satisfies (19) directly implies that the region $\mathcal{R}_i$ between two approximations $\underline{M}_{\tau_i}$ and $\underline{M}_{\tau_{i+1}}$ ($\tau_i < \tau_{i+1}$) can be defined as

$$\mathcal{R}_i := \{x \in \mathbb{R}^n : \mu(x, \tau_i) \leq 0 \wedge \mu(x, \tau_{i+1}) > 0\}. \tag{26}$$

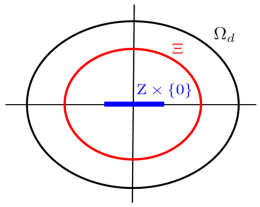

Fig. 6. Sets $\mathrm{Z}\times\{0\}\subset\Xi\subset\Omega_d$.

To determine online to which region does the measured state belong, the controller checks inequalities, such as the ones in (26).

Let us explain the importance of Z, Ξ from Assumption 1. By solving Problem 1, an upper bound $\psi(\xi_0,t)$ is determined according to Lemma V.2 that bounds $\phi(\xi(t;\xi_0))$ as follows:

$$\psi(\xi_0,t)\geq\phi(\xi(t;\xi_0))\quad\forall\xi_0\in\Omega_d \text{ and } \forall t\in[0,\tau_{\xi_0})$$

where τ_{ξ_0} is the time when the trajectory $\xi(t;\xi_0)$ leaves Ω_d [see (21)]. What is needed is to bound $\phi(\xi(t;\xi_0))$ at least until the interevent time $\tau(\xi_0)$ (see Remark 9), i.e., $\tau(\xi_0)<\tau_{\xi_0}$. This is exactly what Assumption 1 offers: trajectories starting from points $\xi_0\in\mathrm{Z}\times\{0\}$ stay in $\Xi\subset\Omega_d$ at least until $\tau(\xi_0)$ (see Fig. 6). In other words, for all points $\xi_0\in\mathrm{Z}\times\{0\}$, we have that $\tau(\xi_0)<\tau_{\xi_0}$ (since $\Xi\subset\Omega_d$) and therefore

$$\psi(\xi_0,t)\geq\phi(\xi(t;\xi_0))\quad\forall\xi_0\in\mathrm{Z}\times\{0\}\text{ and }\forall t\in[0,\tau(\xi_0)]. \tag{27}$$

Regarding the $\{0\}$-part of $\mathrm{Z}\times\{0\}$, note that we only consider initial conditions $\xi_0=(x,0)$, as aforementioned. Finally, transforming $\psi(x,t)$ into $\mu(x,t)$ by incorporating properties (19c) and (19d), (27) becomes (19b). All these statements are formally proven in the Appendix.

VI. Algorithm That Derives Upper Bounds

Although in [1], SOSTOOLS [23] is proposed for deriving the δ_i coefficients, our experience indicates that it is numerically nonrobust regarding solving this particular problem. We present an alternative approach based on a counter-example guided iterative algorithm (see e.g., [25]), which combines linear programming and SMT solvers (e.g., [26]), i.e., tools that verify or disprove first-order logic formulas, such as (24).

Consider the following problem formulation.

Problem Find a vector of parameters Δ such that

$$G(x)\cdot\Delta\leq b(x)\quad\forall x\in\Omega \tag{28}$$

where $\Delta\in\mathbb{R}^p$, $G:\mathbb{R}^n\to\mathbb{R}^{m\times p}$, $b:\mathbb{R}^n\to\mathbb{R}^m$, and Ω is a compact subset of $\mathbb{R}^n$.

For the initialization of the algorithm, a finite subset $\hat{\Omega}$ consisting of samples x_i from the set Ω is obtained. Notice that the relation: $G(x_i)\cdot\Delta\leq b(x_i)\quad\forall x_i\in\hat{\Omega}$ can be formulated as a linear inequality constraint: $\hat{A}\cdot\Delta\leq\hat{b}$, where $\hat{A}=\begin{bmatrix}G^\top(x_1) & G^\top(x_2) & \dots & G^\top(x_i) & \dots\end{bmatrix}^\top$ and $\hat{b}=\begin{bmatrix}b(x_1) & b(x_2) & \dots & b(x_i) & \dots\end{bmatrix}^\top\ \forall x_i\in\hat{\Omega}$. Each iteration of the algorithm consists of the following steps.

1) Obtain a candidate solution $\hat{\Delta}$ by solving the following linear program (LP):
$$\text{minimize}\quad\mathbf{c}^\top\boldsymbol{\Delta},\quad\text{subject to}\quad\hat{\mathbf{A}}\cdot\boldsymbol{\Delta}\leq\hat{\mathbf{b}}$$
where $\mathbf{c}$ can be freely chosen by the user (we discuss meaningful choices later).
2) Employing an SMT solver, check if the candidate solution $\hat{\Delta}$ satisfies the inequality on the original domain, i.e., if $G(x)\cdot\hat{\Delta}\leq b(x)\quad\forall x\in\Omega$.
   1) If $\hat{\Delta}$ satisfies (28), then the algorithm terminates and returns $\hat{\Delta}$ as the solution.
   2) If $\hat{\Delta}$ does not satisfy (28), the SMT solver returns a point $x_c\in\Omega$ where this inequality is violated, i.e., a counter-example. Add x_c to $\hat{\Omega}$ and update accordingly the matrices $\hat{A}$ and $\hat{b}$. Go to step 1.

Note that in b) of step 2, a single constraint is added to the LP of the previous step, i.e., $G(x_c)\cdot\Delta\leq b(x_c)$, by concatenating $G(x_c)$ and $b(x_c)$ to the $\hat{A}$ and $\hat{b}$ matrices, respectively.

In order to solve Problem 1, in particular, we define $\Delta=\begin{bmatrix}\delta_0 & \delta_1 & \dots & \delta_p\end{bmatrix}^\top$, $b(\cdot)=\begin{bmatrix}-\mathcal{L}_F^p\phi(z) & -\varepsilon & \dots & 0\end{bmatrix}^\top$, and

$$G(\cdot)=\begin{bmatrix}-\phi(z) & \dots & -\mathcal{L}_F^{p-1}\phi(z) & -1\\ -\phi(\xi(0;x_0)) & 0 & \dots & -1\\ -1 & 0 & \dots & 0\\ 0 & -1 & \dots & 0\\ 0 & 0 & \ddots & 0\\ 0 & 0 & \dots & -1\end{bmatrix}$$

where $z\in\Omega_d$ and $x_0\in\mathrm{Z}$, with Ω_d and Z as in (23) and Assumption 1, respectively. Hence, the set $\hat{\Omega}$ consists of points $X_i=(z_i,x_{0_i})\in\Omega_d\times\mathrm{Z}$, and after solving the corresponding LP, the SMT solver checks if $G(X)\cdot\hat{\Delta}\leq b(X)\ \ \forall X\in\Omega_d\times\mathrm{Z}$. Finally, intuitively, tighter estimates of $\mathcal{L}_F^p\phi(z)$ could be obtained by minimizing δ_p, and using the other $\mathcal{L}_F^i\phi(z)$ terms in the right-hand side of (20). Hence, $\mathbf{c}=\begin{bmatrix}0 & \dots & 0 & 1\end{bmatrix}$ constitutes a wise choice for the LP. In the following section, numerical examples demonstrate the algorithm's efficiency, alongside the validity of our theoretical results.

Remark 12: It is recommended that the parameter d, which determines the size of Ω_d, is chosen relatively small, in order to help the algorithm terminate faster. Moreover, our experiments indicate that just two initial samples $x_i\in\hat{\Omega}$ are sufficient for the algorithm to terminate relatively quickly. Intuitively, this is because letting the algorithm determine most of the samples itself (by finding the counter-example points) is more efficient than dictating samples a priori. Finally, p should be chosen large enough so that the obtained bound $\mu(\cdot,\cdot)$ is tight, but also small enough so that the dimensionality of the feasibility problem remains small. According to our experience, a choice of $2\leq p\leq 4$ leads to satisfactory results and quick termination of the algorithm, in most cases.

VII. Simulation Results

In the following numerical examples, SOSTOOLS failed to derive upper bounds, as it mistakenly reasoned that Problem 1

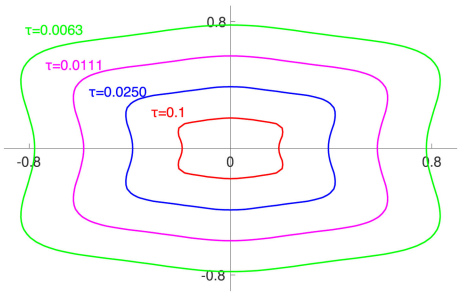

Fig. 7. Approximations of isochronous manifolds of the ETC implementation of (29).

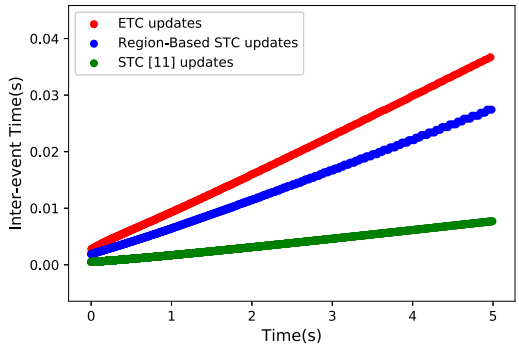

Fig. 8. Time evolution of region-based STC, STC of Anta and Tabuada [11], and ETC interevent times along the trajectory of (29).

is infeasible. The upper bounds were derived by the algorithm proposed earlier.

A. Homogeneous System

In this example, we compare the region-based STC with the STC technique of Anta and Tabuada [11] (which is also computationally light) and with ETC (which constitutes the ideal scenario). Consider the following homogeneous control system:

$$\dot{\zeta}_1 = \zeta_1^3 + \zeta_1\zeta_2^2, \quad \dot{\zeta}_2 = \zeta_1\zeta_2^2 - \zeta_1^2\zeta_2 + \upsilon \tag{29}$$

with $\upsilon(\zeta) = -\zeta_2^3 - \zeta_1\zeta_2^2$. A homogeneous triggering function for an asymptotically stable ETC implementation is

$$\phi(\xi(t;x)) = |\varepsilon(t;x)|^2 - 0.0127^2\sigma^2|\zeta(t;x)|^2, \quad \sigma \in (0,1)$$

where $\xi(\cdot)$ denotes the trajectories of the corresponding extended system (7), $\varepsilon(\cdot)$ is the measurement error (3), and x is the previously sampled state. As in [1], we select $\sigma = 0.3$.

In order to test the proposed region-based STC scheme, Problem 1 is solved by employing the algorithm presented in the previous section. In particular, we set $p = 3, \Omega_d = \{x \in \mathbb{R}^4 : |x| < 0.9\}$, and $\Xi = \mathrm{Z} \times \mathrm{E}$, where $\mathrm{Z} = \{x \in \mathbb{R}^2 : V(x) \leq 0.1\}$, $\mathrm{E} = \{x_0 - x \in \mathbb{R}^2 : \ x, x_0 \in \mathrm{Z}\}$, and $V(x) = \frac{1}{2}x_1^2 + \frac{1}{2}x_2^2$ is a Lyapunov function for the system. Observe that $\Xi \subset \Omega_d$. The coefficients found are $\delta_0 = 0, \delta_1 = 0.1272, \delta_2 = 0$, and $\delta_3 = 0.0191$. In order to construct $\mu(x,t)$ according to (25), we fix $r = 0.29$ and the set $D = \{x \in \mathbb{R}^2 : |x| = r\}$ indeed lies in the interior of Z. The state space is discretized into 348 regions $\mathcal{R}_i$ with corresponding self-triggered interevent times $\tau_{348} = 0.1$ s and $\tau_i = 1.01^{-2}\tau_{i+1}$. Indicatively, four derived approximations of isochronous manifolds are shown in Fig. 7. Observe that the approximations satisfy (13) and (14).

The system is initiated at $x = [1,1]^\top$ and the simulation lasts for 5 s. Fig. 8 compares the time evolution of the interevent times of the region-based STC, the STC proposed in [11] and ETC. In total, ETC triggered 383 times, the region-based STC triggered 554 times, whereas the STC of Anta and Tabuada [11] triggered 2082 times. Given Fig. 8 and the number of total updates for each technique, we can conclude that: first, the region-based STC scheme highly outperforms the STC of Anta and Tabuada [11] and second, the performance of the region-based STC scheme follows closely the ideal performance of ETC while reducing the computational load in the controller.

B. Nonhomogeneous System

Consider the forced Van der Pol oscillator

$$\dot{\zeta}_1(t) = \zeta_2(t), \quad \dot{\zeta}_2(t) = (1 - \zeta_1^2(t))\zeta_2(t) - \zeta_1(t) + \upsilon(t) \tag{30}$$

with $\upsilon(t) = -\zeta_2(t) - (1 - \zeta_1^2(t))\zeta_2(t)$. Assuming an ETC implementation, and homogenizing the system with an auxiliary variable w, according to the procedure presented in [1, Lemma IV.4], the extended system (7) becomes

$$\dot{\xi} = \begin{bmatrix} \xi_2 w^2 \\ (w^2 - \xi_1^2)\xi_2 - \xi_1 w^2 - \epsilon_2 w^2 - (w^2 - \epsilon_1^2)\epsilon_2 \\ 0 \\ -\xi_2 w^2 \\ -(w^2 - \xi_1^2)\xi_2 + \xi_1 w^2 + \epsilon_2 w^2 + (w^2 - \epsilon_1^2)\epsilon_2 \\ 0 \end{bmatrix} \tag{31}$$

where $\xi = [\zeta_1, \zeta_2, w, \varepsilon_1, \varepsilon_2, \varepsilon_w]^\top$, $\epsilon_i = \xi_i + \varepsilon_i$, with ε being the measurement error (3). The homogeneity degree of the extended system is $\alpha = 2$. Observe that the trajectories of the original system (30) coincide with the trajectories of (31), if the initial condition for w is $w_0 = 1$. A triggering function based on the approach of [4] has been obtained in [30]

$$\phi(\zeta(t;x), \varepsilon(t;0)) = \phi(\xi(t;x,w_0)) = W(|\varepsilon|) - V(\xi_1, \xi_2)$$

where $W(|\varepsilon|) = 2.222(\varepsilon_1^2 + \varepsilon_2^2)$ and $V(\xi_1, \xi_2) = 0.0058679\xi_1^2 + 0.0040791\xi_1\xi_2 + 0.0063682\xi_2^2$ is a Lyapunov function for the original system. Note, that $\phi(\xi(t;x,w_0))$ is already homogeneous of degree 1. We fix $\mathrm{Z} = [-0.01, 0.01]^3$ and define the following sets:

$$\Phi = \bigcup_{x_0 \in [-0.01, 0.01]^2} \{x \in \mathbb{R}^2 : W(|x_0 - x|) - V(x_1, x_2) \leq 0\}$$

$$\mathrm{E} = \{x_0 - x \in \mathbb{R}^2 : \ x_0 \in [-0.01, 0.01]^2, \ x \in \Phi\}$$

$$\Xi = \Phi \times [-0.01, 0.01] \times \mathrm{E} \times \{0\}.$$

Notice that Φ is exactly such that for all $x_0 \in [-0.01, 0.01]^2$: $\phi(\xi(t;x_0,w_0)) \leq 0 \Rightarrow \zeta(t;x_0) \in \Phi$. Then, from the definition of E and the observation that w remains constant at all time, it is easily verified that Z and Ξ are compact, contain the origin and satisfy the requirement of Assumption 1.

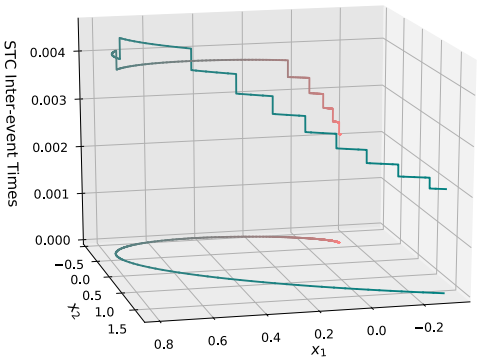

Fig. 9. Evolution of region-based STC interevent times along the trajectory of the forced Van der Pol oscillator.

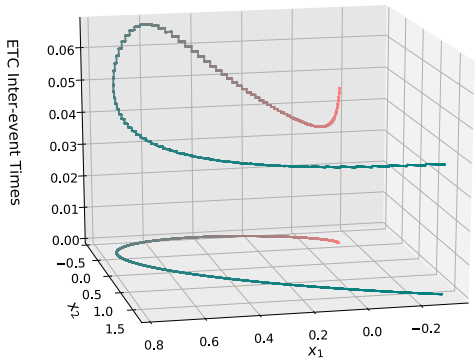

Fig. 10. Evolution of ETC interevent times along the trajectory of the forced Van der Pol oscillator.

Let us compare the region-based STC to the ideal performance of ETC. Solving Problem 1 for $p = 3$, we obtain $\delta_0 = \delta_3 \approx 0$, $\delta_1 \approx 5 \cdot 10^{-7}$, and $\delta_2 \approx 0.00181$. To obtain $\mu(x, w, t)$ as in (25), we fix $r = 0.09$ and $D = \{x \in \mathbb{R}^3 : |x| = r\}$ indeed lies in the interior of Z. The state space is discretized into 126 regions $\mathcal{R}_i$, with $\tau_{126} = 0.01$ s and $\tau_i = 1.05^{-2} \cdot \tau_{i+1}$. The system is initiated at $x = [-0.3, 1.7]^\top$, and the simulation duration is 5 s. In total, the ETC implementation triggered 114 times, whereas the region-based STC implementation triggered 1448 times, which implies that in this particular example, the region-based STC is conservative. Intuitively, the root of conservativeness is the fact that $\mu(x, w, t)$ is now derived to bound the evolution of $\phi(\xi(t; x, w))$ along the trajectories of the extended system (31) in $\mathbb{R}^3$, whereas we only care about the trajectories on the plane $w = 1$.

Figs. 9 and 10 demonstrate the evolution of the sampling times of region-based STC and ETC, respectively, along the trajectory. In particular, the curve on the $x_1 - x_2$ plane is the trajectory of the system, whereas the 3-D curve above the trajectory is the value of the interevent time of the corresponding point on the trajectory. The direction of the trajectory is from the blue-colored points to the red-colored points. In Fig. 9, the intervals for which the interevent time remains constant correspond to segments of the trajectory in which the state vector lies inside one particular region $\mathcal{R}_i$. First, note that in contrast to the previous example, the sampling times do not increase as the system approaches the origin, since the system is not homogeneous and the scaling property (11) does not apply here, i.e., $\phi(\zeta(t; \lambda x)) = \phi(\xi(t; \lambda x, 1)) \neq \lambda^{\theta+1}\phi(\xi(\lambda^\alpha t; x, 1)) = \lambda^{\theta+1}\phi(\zeta(\lambda^\alpha t; x))$. In fact, as stated in [1], the scaling law that applies is

$$\phi(\xi(t; \lambda x, \lambda w)) = \lambda^{\theta+1}\phi(\xi(\lambda^\alpha t; x, w)). \tag{32}$$

However, the similarity of the two figures indicates that the sampling times of the region-based STC approximately follow the trend of the ETC sampling times. This indicates that the approximations of isochronous manifolds determined by $\mu(x, w, t)$ preserve the spatial characteristics of the actual isochronous manifolds of (30). Intuitively, the preservation of the spatial characteristics could be attributed to the fact that $\mu(x, w, t)$ also satisfies (32), which determines the scaling of the isochronous manifolds of the homogenized system (31) along its homogeneous rays. Besides, note that the isochronous manifolds of the original system (30) are the intersections of the isochronous manifolds of (31) with the $w = 1$-plane.

Remark 13: This simulation demonstrates that as mentioned in Remark 2, the results presented in this article are transferable to any smooth, not necessarily homogeneous, system.

VIII. Conclusion and Future Work

In this article, a novel STC policy that enables a tradeoff between online computations and updates was presented. The simulation results indicate that the scheme performs very well in the case of homogeneous systems. However, it was also shown that for nonhomogeneous systems, the performance deteriorated. Thus, future research will consider ways of improving the performance for nonhomogeneous systems. Furthermore, we aim at addressing perturbed and noisy nonlinear systems. Finally, the approximations of isochronous manifolds could be employed to derive a state-space discretization in accordance to what is proposed in [31], in order to synthesize a scheduling framework for networks of nonlinear ETC systems.

Appendix

To conduct the proofs of the previously presented lemmas and theorems, we first introduce some preliminary concepts.

A. Higher Order Differential Inequalities

Definition VIII.1 (Type W^* functions [24]): The function $g : \mathbb{R}^n \to \mathbb{R}$ is said to be of type W^* on a set $S \subseteq \mathbb{R}^n$ if $g(x) \leq g(y)$ for all $x, y \in S$ such that $x_n = y_n$, $x_i \leq y_i$ $(i = 1, 2, \ldots, n-1)$, where x_i and y_i denote the ith component of the x and y vectors, respectively.

Definition VIII.2 (Right Maximal Solution [24]): Consider the pth order differential equation

$$u^{(p)}(t) = g(t, u(t), \dot{u}(t), \ldots, u^{(p-1)}(t)) \tag{33}$$

where $u : \mathbb{R}^+ \to \mathbb{R}$ and $g(\cdot)$ is continuous on $[0, T] \times \mathbb{R}^p$. A solution $u_m(t; t_0, U_m)$, where t_0 is the initial time instant and $U_m \in \mathbb{R}^p$ is the vector of initial conditions, is called a right maximal solution of (33) on an interval $[t_0, \alpha) \subset [0, T]$ if

$$u^{(i)}(t; t_0, U_0) \leq u_m^{(i)}(t; t_0, U_m), \quad t \in [t_0, \alpha) \cap [t_0, \alpha^*)$$

for any other solution $u(t;t_0,U_0)$ with initial condition $U_0 \preceq U_m$ defined on $[t_0,\alpha^*)$, for all $i=0,1,2,\dots,m-1$.

Lemma VIII.1 (Higher Order Comparison Lemma [24]): Consider a system of first-order differential equations

$$\dot{\zeta}(t) = f(t,\zeta(t)). \tag{34}$$

Let $\upsilon : D_r \to \mathbb{R}$ and let $\upsilon \in \mathcal{C}^p$, $f \in \mathcal{C}^{p-1}$ on D_r, where $D_r = \{(t,x)|0 \le t \le T < +\infty, |x| < r\}$. Let $g(\cdot)$ of (33) be of type W^* on $S \subseteq \mathbb{R}^{p+1}$ for each t, where

$$S = \Big\{ \Big(t, \upsilon(t,\zeta(t)), \dot{\upsilon}(t,\zeta(t)), \dots, \upsilon^{(p-1)}(t,\zeta(t))\Big) \mid (t,\zeta(t)) \in D_r \Big\}$$

and

$$\upsilon^{(i)}(t,\zeta(t)) = \frac{\partial \upsilon^{(i-1)}(t,\zeta(t))}{\partial t} + \frac{\partial \upsilon^{(i-1)}(t,\zeta(t))}{\partial \zeta(t)} \cdot f(t,\zeta(t)).$$

Assume that

$$\upsilon^{(p)}(t,\zeta(t)) \le g(t,\upsilon(t,\zeta(t)),\dot{\upsilon}(t,\zeta(t)),\dots,\upsilon^{(p-1)}(t,\zeta(t)))$$

for all $(t,\zeta(t)) \in D_r$. Let J denote the maximal interval of existence of the right maximal solution $u_m(t;0,U_m)$ of (33). If $\upsilon^{(i)}(0,\zeta_0) = u_m^{(i)}(0;0,U_m)$ $(i=0,1,2,\dots,p-1)$, where $u_m^{(i)}(0;0,U_m)$ are the components of the initial condition U_m of $u_m(t;0,U_m)$, then

$$\upsilon^{(i)}(t,\zeta(t;0,\zeta_0)) \le u_m^{(i)}(t;0,U_m), \quad t \in J \cap [0,T]$$

for all $i=0,1,2,\dots,p-1$.

B. Monotone Systems

Definition VIII.3 (Monotone System[32]): Consider a system

$$\dot{\zeta}(t) = f(\zeta(t)). \tag{35}$$

The system (35) is called monotone if

$$\zeta_0 \preceq \zeta_1 \Rightarrow \zeta(t;t_0,\zeta_0) \preceq \zeta(t;t_0,\zeta_1).$$

Proposition VIII.1 (see [32]): Consider the system (35). If the off-diagonal entries of the Jacobian $\frac{\partial f}{\partial \zeta}$ are nonnegative, then the system (35) is monotone.

C. Technical Proofs

Proof of Theorem V.1 Define $\tau^{\downarrow}(x) = \inf\{t>0 : \mu(x,t) = 0\}$. Equation (19d) implies that $\mu(x,\tau^{\downarrow}(x)) = 0$ is the only zero crossing of $\mu(x,t)$ w.r.t. t for any given x. Hence

$$\underline{M}_{\tau_\star} = \{x \in \mathbb{R}^n : \mu(x,\tau_\star) = 0\} = \{x \in \mathbb{R}^n : \tau^{\downarrow}(x) = \tau_\star\}.$$

Equations (19c) and (19d) imply that $\underline{M}_{\tau_\star}$ satisfies (13) and (14) (see Remark 5).

It is left to prove that $\underline{M}_{\tau_\star}$ is an inner approximation of $M_{\tau_\star}$. Notice that $\phi(\xi(\tau(x);x)) = 0$ together with (19b) and (19a) imply that the first zero crossing of $\mu(x,t)$ happens before the one of the triggering function

$$\tau^{\downarrow}(x) \le \tau(x). \tag{36}$$

Furthermore, (19c) implies that $\tau_{\downarrow}(x)$ also satisfies the scaling law (10) (the proof for this argument is the exact same to the one derived in [11] for the scaling laws of interevent times). The fact that both $\tau_{\downarrow}(x)$ and $\tau(x)$ satisfy (10), i.e., they are strictly decreasing functions along homogeneous rays, alongside (36) implies that: $\tau(x_1) = \tau^{\downarrow}(x_2) = \tau_\star \Rightarrow |x_1| \ge |x_2|$, for all x_1, x_2 on a homogeneous ray. Thus, since $\underline{M}_{\tau_\star}$ satisfies (13), we get that for all $x \in \underline{M}_{\tau_\star}$

$$\exists! \kappa_x \ge 1 \text{ s.t. } \kappa_x x \in M_{\tau_i} \text{ and } \nexists \lambda_x \in (0,1) \text{ s.t. } \lambda_x x \in M_{\tau_i}.$$

■

Proof of Lemma V.2 Introduce the following linear system:

$$\dot{\chi} = \begin{bmatrix} 0 & 1 & 0 & \dots & 0 & 0 \\ 0 & 0 & 1 & \dots & 0 & 0 \\ \vdots & \vdots & & \ddots & \vdots & \vdots \\ 0 & 0 & 0 & \dots & 1 & 0 \\ 0 & 0 & 0 & \dots & 0 & 1 \\ \delta_0 & \delta_1 & \delta_2 & \dots & \delta_{p-2} & \delta_{p-1} \end{bmatrix} \chi + \begin{bmatrix} 0 \\ \vdots \\ 0 \\ \delta_p \end{bmatrix}. \tag{37}$$

Notice that (37) represents the pth order differential equation $\chi^{(p)} = \sum_{i=0}^{p-1} \delta_i \chi^{(i)} + \delta_p$. The proof makes use of Lemma VIII.1. Using the notation of Lemma VIII.1, we identify

$$\upsilon(t,\xi(t)) \equiv \phi(\xi(t)) \quad \forall \xi(t) \in \Omega_d$$
$$f(t,\xi(t)) \equiv F(\xi(t)) \quad \forall \xi(t) \in \Omega_d$$
$$g\left(t, v, v', ..., v^{(p-1)}\right) \equiv \sum_{i=0}^{p-1} \delta_i v^{(i)} + \delta_p.$$

For $t > \tau_{\xi_0}$, $\xi(t;\xi_0)$ may not belong to Ω_d. Thus, $\upsilon(\cdot)$ is well defined only in the interval $[0,\tau_{\xi_0})$. Since $\delta_i \ge 0$ for all i, g is of type W^* in $\mathbb{R}^+ \times \mathbb{R}^p$. Moreover, it is clear that $\upsilon \in C^p$ and $f \in C^{p-1}$ on $[0,\tau_{\xi_0}) \times \Omega_d$. Inequality (20) translates to $\upsilon^{(p)}(t,z) \le g(t,v,v',...,v^{(p-1)})$ for $(t,z) \in [0,\tau_{\xi_0}) \times \Omega_d$.

Furthermore, according to Proposition VIII.1, the linear system (37) is monotone, since all off-diagonal entries of its Jacobian are nonnegative ($\delta_i \ge 0$ for all i). This implies that any solution of (37) is a right maximal solution, and its maximal interval of existence is $J = [0,+\infty)$. Consider the solution $\chi(t;X(\xi_0))$, where $X(\xi_0) = \begin{bmatrix} \phi(\xi_0) & \mathcal{L}_F\phi(\xi_0) & \dots & \mathcal{L}_F^{p-1}\phi(\xi_0) \end{bmatrix}^\top$. Observe that the components of the initial condition $X(\xi_0)$ and $\mathcal{L}_F^i\phi(z)$ $(i=0,1,2,\dots,p-1)$ are equal. All conditions of Lemma (VIII.1) are satisfied. Thus, we can conclude that for all $\xi_0 \in \Omega_d$

$$\phi(\xi(t;\xi_0)) \le \chi_1(t;X(\xi_0)) \quad \forall t \in [0,\tau_{\xi_0}).$$

Notice that $\psi_1(y(\xi_0),t) = \chi_1(t;X(\xi_0))$ for all t. Hence, $\phi(\xi(t;\xi_0)) \le \psi_1(y(\xi_0),t) \quad \forall t \in [0,\tau_{\xi_0})$. ■

To prove Theorem V.3, we first derive the following results.

Proposition VIII.2: Consider coefficients δ_i $(i=0,1,...,p)$ solving Problem 1, and define an upper bound $\psi_1(x,t)$ of the triggering function $\phi(\xi(t;x))$ as dictated in Lemma V.2. Let

$$\eta_1(x,t) := Ce^{At}\eta(x,0) \tag{38}$$

where A is as in (22), $C = \begin{bmatrix} 1 & 0 & \dots & 0 \end{bmatrix}$, and

$$\eta(x,0) := \begin{bmatrix} \phi\left((x,0)\right) \\ \max\left(\mathcal{L}_f \phi\left((x,0)\right), 0\right) \\ \vdots \\ \max\left(\mathcal{L}_f^{p-1} \phi\left((x,0)\right), 0\right) \\ \delta_p \end{bmatrix}. \tag{39}$$

The function $\eta_1(x,t)$ satisfies

$$\eta_1(x,t) \geq \phi(\xi(t;x)) \quad \forall t \in [0, \tau(x)] \text{ and } \forall x \in \mathrm{Z}. \tag{40}$$

Proof: Notice that η_1 is the first component of the solution $\eta(x,t)$ to the same linear dynamical system (22) as ψ, with initial condition: $\psi(x,0) \preceq \eta(x,0)$. Since the system (22) is monotone, according to Proposition VIII.1, the following holds:

$$\eta_1(x,t) \geq \psi_1(x,t) \geq \phi(\xi(t;x)) \quad \forall t \in [0, \tau_{\xi_0}) \text{ and } \forall x \in \mathrm{Z}$$

since $x \in \mathrm{Z} \Rightarrow \xi_0 = (x,0) \in \Xi \subset \Omega_d$. By the definition of Ξ in Assumption 1, $\xi(t;x) \in \Xi$ for all $t \in [0, \tau(x)]$. But τ_{ξ_0} is defined in (21) as the escape time of $\xi(t;x)$ from Ω_d, and $\Xi \subset \Omega_d$; i.e., $\tau(x) < \tau_{\xi_0}$. Thus, (40) is satisfied. ■

Proposition VIII.3: The function $\eta_1(x,t)$ of (38) is strictly increasing w.r.t. t for all $t > 0$.

Proof: In the following, $\eta_1^{(i)}(x,t)$ denotes the ith derivative of $\eta_1(x,t)$ w.r.t. t. At $t = 0$, initial condition (39) implies that $\eta_1^{(i)}(x,0) \geq 0$ for all $i = 1, \dots, p-1$. For $\eta_1^{(p)}(x,0)$

$$\eta_1^{(p)}(x,0) = \sum_{i=0}^{p-1} \delta_i \eta_{i+1}(x,0) + \delta_p \geq \delta_0 \phi\left((x,0)\right) + \delta_p > 0$$

since $\eta_{i+1}(x,0) \geq 0$ for all $i = 0, \dots, p-1$, and (24b) and (24c) hold. Differentiating $\eta_1^{(p)}$ w.r.t. t, we get

$$\eta_1^{(p+1)}(x,0) = \sum_{i=0}^{p-1} \delta_i \eta_1^{(i+1)}(x,0) \geq 0.$$

Similarly, $\eta_1^{(i)}(x,0) \geq 0$, for all i. Hence, $\eta_1^{(i)}(x,0) \geq 0$ for all $i \in \mathbb{N} - \{0\}$, and, in particular, $\eta_1^{(p)}(x,0) > 0$. This implies that the function $\eta_1(x,t)$ is strictly increasing for all $t > 0$. ■

We are ready to prove Theorem V.3.

Proof of Theorem V.3: First, notice that $\mu(x,t)$ satisfies (19c), by construction. Let $D = \{x \in \mathbb{R}^n : |x| = r\}$, with $r > 0$ such that $D \subset \mathrm{Z}$. Notice that for $x \in D$: $\mu(x,t) = \eta(x,t)$. Thus, according to Proposition VIII.2

$$\mu(x,t) = \eta_1(x,t) \geq \phi(\xi(t;x)) \quad \forall t \in [0, \tau(x)] \text{ and } \forall x \in D. \tag{41}$$

Consider now any $x_0 \in \mathbb{R}^n - \{0\}$ and a $\lambda > 0$ such that $x_D = \lambda x_0 \in D$. Employing (19c), (11), and (41), we get

$$\mu(x_D,t) \geq \phi(\xi(t;x_D)) \quad \forall t \in [0, \tau(x_D)] \iff$$
$$\mu(x_0, \lambda^\alpha t) \geq \phi(\xi(\lambda^\alpha t; x_0)) \quad \forall t \in [0, \tau(x_D)] \iff$$
$$\mu(x_0,t) \geq \phi(\xi(t;x_0)) \quad \forall x_0 \in \mathbb{R}^n - \{0\} \text{ and } t \in [0, \tau(x_0)]$$

since $\lambda^\alpha \tau(x_D) = \tau(x_0)$. Thus, $\mu(x,t)$ satisfies (19b).

It remains to be shown that $\mu(x,t)$ satisfies (19d). Notice that $\mu(x,0) = \phi((x,0)) < 0$ for all $x \in \mathbb{R}^n - \{0\}$. Moreover, since (19b) holds, we get that

$$\mu(x, \tau(x)) \geq \phi(\xi(\tau(x); x)) = 0.$$

From Assumption 1, we have that $\tau(x)$ always exists. Thus, for all $x \in \mathbb{R}^n - \{0\}$, there exists $\tau_\downarrow(x) > 0$ such that $\mu(x, \tau_\downarrow(x)) = 0$. Moreover, since $\mu(x,t) = \eta(x,t)$ for $x \in D$, then according to Proposition VIII.3, $\mu(x,t)$ is strictly increasing w.r.t. t for all $t > 0$ and for all $x \in D$. Finally, incorporating (19c), we get that: $\mu(x,t)$ is strictly increasing w.r.t. t for all $t > 0$ and for all $x \in \mathbb{R}^n - \{0\}$; i.e., $\tau_\downarrow(x)$ is unique. Thus, $\mu(x,t)$ satisfies (19d). ■

D. Nonhomogeneous Systems

As stated in Remark 2, in [1], a procedure is proposed that renders any smooth nonlinear system homogeneous of degree $\alpha > 0$, by embedding it to higher dimensions and adding an extra variable w, with dynamics $\dot{w} = 0$. Specifically, a nonlinear system

$$\dot{\zeta}(t) = f(\zeta(t)) \tag{42}$$

with $\zeta(t) \in \mathbb{R}^n$ is homogenized as follows:

$$\begin{bmatrix} \dot{\zeta}(t) \\ \dot{w}(t) \end{bmatrix} = \begin{bmatrix} w^{\alpha+1} f_1(w^{-1}\zeta(t)) \\ w^{\alpha+1} f_2(w^{-1}\zeta(t)) \\ \vdots \\ w^{\alpha+1} f_n(w^{-1}\zeta(t)) \\ 0 \end{bmatrix} = \tilde{f}(\zeta(t), w(t)). \tag{43}$$

Likewise, an ETC system (7) is homogenized by introducing w and the corresponding dummy measurement error ε_w as

$$\dot{\xi}(t) = \begin{bmatrix} \dot{\zeta}(t) \\ \dot{w}(t) \\ \dot{\varepsilon}_\zeta(t) \\ \dot{\varepsilon}_w(t) \end{bmatrix} = \begin{bmatrix} \tilde{f}(\zeta(t), \varepsilon_z(t), w(t)) \\ 0 \\ -\tilde{f}(\zeta(t), \varepsilon_z(t), w(t)) \\ 0 \end{bmatrix} = F(\xi(t)) \tag{44}$$

where $\tilde{f}(\zeta(t), \varepsilon_z(t), w(t))$ is obtained as in (43).

An example of the use of the homogenization procedure is demonstrated in Section VII-B. Similarly, one can homogenize a nonhomogeneous triggering function $\phi(\zeta(t;x_0), \varepsilon_\zeta(t;0))$ as: $\tilde{\phi}(\xi(t;x_0,w_0)) = w^{\theta+1}\phi(w^{-1}\zeta(t;x_0), w^{-1}\varepsilon_\zeta(t;0))$. Observe that the trajectories of the original system (42) with initial condition $x \in \mathbb{R}^n$ coincide with the ones of (43) with initial condition $(x,1) \in \mathbb{R}^{n+1}$, i.e., on the hyperplane $w = 1$. Hence, the interevent times of the original system $\tau(x)$ coincide with the interevent times $\tau((x,1))$ of (43). Consequently, in order to apply the proposed region-based STC scheme to a nonhomogeneous nonlinear system, we first homogenize it by embedding it to $\mathbb{R}^{n+1}$, and then derive inner approximations of isochronous manifolds of the extended system (43), by replacing x with (x,w) in (25).

However, a technical detail arises that needs to be emphasized. Most triggering functions that are designed for asymptotic stabilization of the origin (e.g., [4]) satisfy $\phi((0,0)) = 0$. Thus,

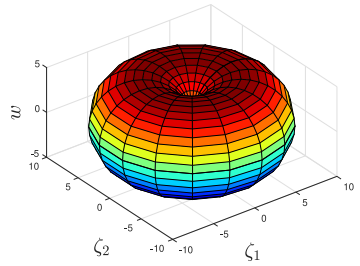

Fig. 11. Inner approximation $\underline{M}_{\tau_\star}$ of isochronous manifolds of a homogenized system.

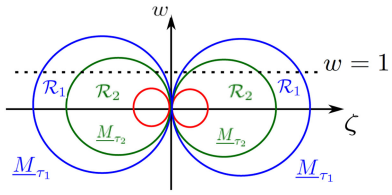

Fig. 12. Discretization of the state space of a homogenized system into regions $\mathcal{R}_i$ delimited by inner approximations $\underline{M}_{\tau_i}$ (colored lines) of isochronous manifolds.

deriving the function $\mu(x,w,t)$ as in Theorem V.3 for the extended system (43), results for all points $(0,w) \in \mathbb{R}^{n+1} - \{0\}$ on the w-axis in

$$\mu(0,w,t) = C(\tfrac{|w|}{r})^{\theta+1} e^{A(\frac{|w|}{r})^{\alpha} t} \begin{bmatrix} 0 \\ \max\left(\mathcal{L}_f \phi\left((0,0)\right), 0\right) \\ \vdots \\ \max\left(\mathcal{L}_f^{p-1} \phi\left((0,0)\right), 0\right) \\ \delta_p \end{bmatrix}.$$

This implies that for all these points: $\mu(0,w,t) > 0$ for all $t > 0$. Hence, the w-axis does not belong to any inner approximation $\underline{M}_{\tau_\star} = \{(x,w) \in \mathbb{R}^{n+1} : \mu(x,w,\tau_\star) = 0\}$ of isochronous manifolds. In other words, all inner approximations $\underline{M}_{\tau_\star}$ are punctured by the w-axis and obtain a singularity at the origin, as shown in Fig. 11. Consequently, given a finite set of times $\{\tau_1, \ldots, \tau_q\}$, discretizing the state space of the extended system into regions $\mathcal{R}_i$ delimited by inner approximations $\underline{M}_{\tau_i}$ will always result in a neighborhood around the w-axis not belonging to any region $\mathcal{R}_i$, as depicted in Fig. 12. This implies that a neighborhood around the origin of the original system (42), which is mapped to a subset of the hyperplane $w = 1$ around the w-axis in the augmented space $\mathbb{R}^{n+1}$, is not contained to any region $\mathcal{R}_i$. Thus, no STC interevent time can be assigned to the points of this neighborhood.

However, note that this neighborhood can be made arbitrarily small, by selecting a sufficiently small time τ_1 for the outermost inner approximation $\underline{M}_{\tau_1}$. Thus, in order to apply the region-based STC scheme in practice, first we make this neighborhood arbitrarily small, and then we treat it differently by associating it to a sampling time that can be designed e.g., according to periodic sampling techniques that guarantee stability (e.g., [33]). In the numerical example of Section VII-B, we completely neglect this region, as it was so small that it was not even reached during the simulation.

Remark 14: Note that as the w-axis acts as a singularity for both the isochronous manifolds $M_{\tau_\star}$ (the actual interevent times there are technically 0, and in practice they could be anything) and their inner approximations $\underline{M}_{\tau_\star}$, the inner approximations might look very different than the actual manifolds near the w-axis.

Remark 15: The aforementioned technical issue does not arise in cases where $\phi((0,0)) \neq 0$. Such an example is the widely used mixed-triggering function $\phi(\xi(t)) = |\varepsilon_\zeta(t)|^2 - \sigma|\zeta(t)|^2 - \epsilon^2$ (e.g., [34]), where $\sigma > 0$ is appropriately chosen and $\epsilon > 0$.

ACKNOWLEDGMENT

The authors would like to thank C. F. Verdier for assisting to the implementation of the algorithm described in Section VI, A. Anta and P. Tabuada for fruitful discussions on this article, and X. Xu for pointing out references [24] and [29].

REFERENCES

[1] A. Anta and P. Tabuada, "Exploiting isochrony in self-triggered control," *IEEE Trans. Autom. Control*, vol. 57, no. 4, pp. 950–962, Apr. 2012.
[2] K.-E. Åarzén, "A simple event-based PID controller," *IFAC Proc. Vol.*, vol. 32, no. 2, pp. 8687–8692, 1999.
[3] W. Heemels *et al.*, "Asynchronous measurement and control: a case study on motor synchronization," *Control Eng. Pract.*, vol. 7, no. 12, pp. 1467–1482, 1999.
[4] P. Tabuada, "Event-triggered real-time scheduling of stabilizing control tasks," *IEEE Trans. Autom. Control*, vol. 52, no. 9, pp. 1680–1685, Sep. 2007.
[5] M. Mazo and P. Tabuada, "Decentralized event-triggered control over wireless sensor/actuator networks," *IEEE Trans. Autom. Control*, vol. 56, no. 10, pp. 2456–2461, Oct. 2011.
[6] A. Girard, "Dynamic triggering mechanisms for event-triggered control," *IEEE Trans. Autom. Control*, vol. 60, no. 7, pp. 1992–1997, Jul. 2015.
[7] B. A. Khashooei, D. J. Antunes, and W. P. M. H. Heemels, "An event-triggered policy for remote sensing and control with performance guarantees," in *Proc. IEEE Conf. Decis. Control*, 2015, pp. 4830–4835.
[8] D. Lehmann and J. Lunze, "Event-based output-feedback control," in *Mediterranean Conf. Control Automat.*, 2011, pp. 982–987.
[9] J. Lunze and D. Lehmann, "A state-feedback approach to event-based control," *Automatica*, vol. 46, no. 1, pp. 211–215, 2010.
[10] M. Velasco, J. Fuertes, and P. Marti, "The self triggered task model for real-time control systems," in *Proc. Work Prog. Session 24th IEEE Real-Time Syst. Symp.*, 2003, vol. 384, pp. 67–70.
[11] A. Anta and P. Tabuada, "To sample or not to sample: Self-triggered control for nonlinear systems," *IEEE Trans. Autom. Control*, vol. 55, no. 9, pp. 2030–2042, Sep. 2010.
[12] M. D. Di Benedetto, S. Di Gennaro, and A. D'innocenzo, "Digital self-triggered robust control of nonlinear systems," *Int. J. Control*, vol. 86, no. 9, pp. 1664–1672, 2013.
[13] U. Tiberi and K. H. Johansson, "A simple self-triggered sampler for perturbed nonlinear systems," *Nonlinear Anal.: Hybrid Syst.*, vol. 10, no. 1, pp. 126–140, 2013.
[14] M. Mazo, Jr, A. Anta, and P. Tabuada, "An ISS self-triggered implementation of linear controllers," *Automatica*, vol. 46, no. 8, pp. 1310–1314, 2010.
[15] M. Mazo, A. Anta, and P. Tabuada, "On self-triggered control for linear systems: Guarantees and complexity," in *Proc. Eur. Control Conf.*, 2009, pp. 3767–3772.
[16] D. Tolic, R. G. Sanfelice, and R. Fierro, "Self-triggering in nonlinear systems: A small gain theorem approach," in *Proc. Mediterranean Conf. Control Automat.*, 2012, pp. 941–947.
[17] T. Gommans, D. Antunes, T. Donkers, P. Tabuada, and M. Heemels, "Self-triggered linear quadratic control," *Automatica*, vol. 50, no. 4, pp. 1279–1287, 2014.

[18] C. Fiter, L. Hetel, W. Perruquetti, and J.-P. Richard, "A state dependent sampling for linear state feedback," *Automatica*, vol. 48, no. 8, pp. 1860–1867, 2012.
[19] X. Wang and M. D. Lemmon, "Self-triggered feedback control systems with finite-gain l_2 stability," *IEEE Trans. Autom. Control*, vol. 54, no. 3, pp. 452–467, Mar. 2009.
[20] X. Wang and M. D. Lemmon, "Self-triggering under state-independent disturbances," *IEEE Trans. Autom. Control*, vol. 55, no. 6, pp. 1494–1500, Jun. 2010.
[21] D. Theodosis and D. V. Dimarogonas, "Self-triggered control under actuator delays," in *Proc. IEEE Conf. Decis. Control*, 2018, pp. 1524–1529.
[22] W. P. M. H. Heemels, K. H. Johansson, and P. Tabuada, "An introduction to event-triggered and self-triggered control," in *Proc. IEEE Conf. Decis. Control*, 2012, pp. 3270–3285.
[23] S. Prajna, A. Papachristodoulou, and P. A. Parrilo, "Introducing SOSTOOLS: A general purpose sum of squares programming solver," in *Proc. 41st IEEE Conf. Decis. Control*, 2002, vol. 1, pp. 741–746.
[24] R. Gunderson, "A comparison lemma for higher order trajectory derivatives," in *Proc. Amer. Math. Soc.*, 1971, pp. 543–548.
[25] J. Kapinski, S. Sankaranarayanan, J. V. Deshmukh, and N. Archiga, "Simulation-guided Lyapunov analysis for hybrid dynamical systems," in *Proc. 17th Int. Conf. Hybrid Syst.: Comput. Control*, 2014, pp. 133–142.
[26] S. Gao, S. Kong, and E. M. Clarke, "dReal: An SMT solver for nonlinear theories over the reals," in *Proc. Int. Conf. Autom. Deduction*, 2013, pp. 208–214.
[27] M. Kawski, "Geometric homogeneity and stabilization," in *Nonlinear Control Syst. Des.*, 1995, pp. 147–152.
[28] M. Krstic and P. V. Kokotovic, "Lean backstepping design for a jet engine compressor model," in *Proc. 4th IEEE Conf. Control Appl.*, 1995, pp. 1047–1052.
[29] V. Meigoli and S. K. Y. Nikravesh, "A new theorem on higher order derivatives of Lyapunov functions," *ISA Trans.*, vol. 48, no. 2, pp. 173–179, 2009.
[30] R. Postoyan, P. Tabuada, D. Nesic, and A. A. Martinez, "A framework for the event-triggered stabilization of nonlinear systems," *IEEE Trans. Autom. Control*, vol. 60, no. 4, pp. 982–996, Apr. 2015.
[31] A. Kolarijani and M. Mazo, "Formal traffic characterization of LTI event-triggered control systems," *IEEE Trans. Control of Netw. Syst.*, vol. 5, no. 1, pp. 274–283, Mar. 2018.
[32] H. L. Smith, *Monotone Dynamical Systems: An Introduction to the Theory of Competitive and Cooperative Systems*. Providence, RI, USA: Amer. Math. Soc., 2008, no. 41.
[33] D. Carnevale, A. R. Teel, and D. Nesic, "A Lyapunov proof of an improved maximum allowable transfer interval for networked control systems," *IEEE Trans. Autom. Control*, vol. 52, no. 5, pp. 892–897, May 2007.
[34] T. Liu and Z.-P. Jiang, "A small-gain approach to robust event-triggered control of nonlinear systems," *IEEE Trans. Autom. Control*, vol. 60, no. 8, pp. 2072–2085, Aug. 2015.

Giannis Delimpaltadakis (Student Member, IEEE) received his Diploma (joint B.Sc. and M.Sc.) in electrical and computer engineering from the National Technical University of Athens, Greece, in 2017. He is currently working toward the Ph.D. degree at the Delft Center for Systems and Control, Delft University of Technology, Delft, The Netherlands. His on-going work primarily focuses on scheduling of communication traffic in networks of event-triggered control systems.

His research interests include event-triggered and self-triggered control, nonlinear systems, and networked control systems.

Manuel Mazo, Jr. (Senior Member, IEEE) received the Telecommunications Engineering (Ingeniero) degree from the Polytechnic University of Madrid, Madrid, Spain, in 2003, the Civilingenjör degree in electrical engineering from the KTH Royal Institute of Technology, Stockholm, Sweden, in 2003, and the M.Sc. and Ph.D. degrees in electrical engineering from the University of California, Los Angeles, Los Angeles, CA, USA, in 2007 and 2010, respectively.

He is currently an Associate Professor with the Delft Center for Systems and Control, Delft University of Technology, Delft, The Netherlands. Between 2010 and 2012, he held a joint Postdoctoral position with the University of Groningen and the Innovation Centre for Advanced Sensors and Sensor Systems, The Netherlands. His main research interest include the formal study of problems emerging in modern control system implementations, and, in particular, the study of networked control systems and the application of formal verification and synthesis techniques to control.

Dr. Mazo, was the recipient of the University of Newcastle Research Fellowship in 2005, the Spanish Ministry of Education/UCLA Fellowship from 2005 to 2009, the Henry Samueli Scholarship from the UCLA School of Engineering and Applied Sciences in 2007 and 2008, and an ERC Starting Grant in 2017.